ACS APPLIED MATERIALS & INTERFACES

Research Article

www.acsami.org

Synthesis of One-Dimensional SiC Nanostructures from a Glassy Buckypaper

Mengning Ding[†,‡] and Alexander Star*[,†,‡]

[†]U.S. Department of Energy, National Energy Technology Laboratory, Pittsburgh, Pennsylvania 15236, United States

[‡]Department of Chemistry, University of Pittsburgh, Pittsburgh, Pennsylvania 15260, United States

Supporting Information

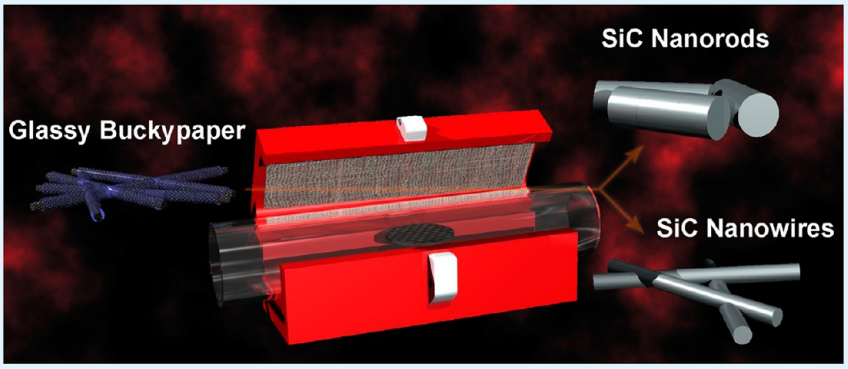

ABSTRACT: A simple and scalable synthetic strategy was developed for the fabrication of one-dimensional SiC nanostructures—nanorods and nanowires. Thin sheets of single-walled carbon nanotubes (SWNTs) were prepared by vacuum filtration and were washed repeatedly with sodium silicate (Na_2SiO_3) solution. The resulting "glassy buckypaper" was heated at 1300−1500 °C under Ar/H_2 to allow a solid state reaction between C and Si precursors to form a variety of SiC nanostructures. The morphology and crystal structures of SiC nanorods and nanowires were characterized using scanning electron microscopy (SEM), high-resolution transmission electron microscopy (HR-TEM), energy-dispersive X-ray spectroscopy (EDX), electron diffraction (ED), and X-ray diffraction (XRD) techniques. Furthermore, electrical conductance measurements were performed on SiC nanorods, demonstrating their potential applications in high-temperature sensors and control systems.

KEYWORDS: *SiC nanorods, SiC nanowires, carbon nanotubes, silicate, high-temperature sensors*

1. INTRODUCTION

Silicon carbide (SiC) has been widely recognized as a versatile material with tremendous industrial applications because of its unique mechanical, electrical, and thermal properties.[1] The synthesis of SiC has been extensively explored during the past century, and many general synthetic methods have been summarized in great detail.[2,3] Recently, the research focus has been shifted to the fabrication of one-dimensional (1-D) SiC nanostructures because of their potential applications in nanoelectronics as analogues to carbon nanotubes[4] and Si nanowires.[5] Due to their high thermal stability, chemical inertness, and high mechanical strength, 1-D SiC nanostructures are especially promising for the employment in a high power, high frequency, and high temperature environment.[6,7] Growth of 1-D SiC nanostructures has been carried out by a variety of methods including chemical vapor deposition (CVD),[8−12] arc discharge,[13,14] pyrolysis of polysilazane,[15] crystal growth from solution,[16,17] carbothermal reduction,[18,19] vapor−solid reaction between gaseous carbon and Si substrate,[20,21] and a confined reaction between Si precursors and carbon nanofibers[22−24] or carbon nanotubes (CNTs).[25−30] This latter approach has its own advantages due to the easy processing of free-standing carbon nanotube samples and the increasing industrial production and declining cost of carbon nanotubes. Lieber and co-workers first demonstrated the synthesis of SiC nanorods through the reaction between carbon nanotubes and gaseous SiO or SiI_4.[25] In this approach CNTs acted as both the carbon source and template for the growth of the one-dimensional nanostructures. Similar approaches were reported following this work with different Si sources including sputter-coated Si,[26] SiO vapor,[27−29] and Si vapor.[30] Despite the successful synthesis of one-dimensional SiC nanostructures, all of these methods required the generation of toxic Si-containing vapor that complicated the manufacturing process and caused significant waste of the Si precursors. Here we report a facile and scalable approach where adsorbed silicate was employed as the Si precursor to react with carbon nanotube templates. The silicate was introduced by washing the "buckypaper" of carbon nanotubes with aqueous sodium silicate solution. Since sodium silicate is also known as

Received: July 26, 2012
Accepted: February 21, 2013
Published: February 21, 2013

Scheme 1. Synthesis of One-Dimensional (1-D) SiC Nanostructures from a SWNT−Silicate Composite ("Glassy Buckypaper")[a]

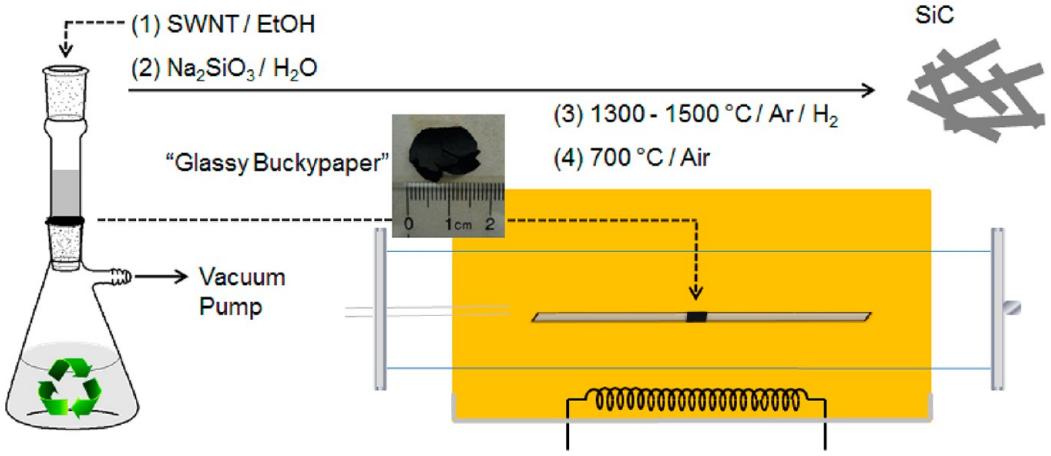

[a]"Glassy buckypaper" was prepared using vacuum filtration of (1) SWNT suspension in ethanol, followed by (2) continuous washing with sodium silicate solution. The "glassy buckypaper" was further (3) calcinated at high temperature in a tube furnace and after (4) burning unreacted carbon in air affording SiC 1-D nanostructures.

water glass, the resulting SWNT−silicate film is designated here as "glassy buckypaper". This "glassy buckypaper" was further used to produce the SiC nanostructures after high-temperature calcination. The solution-based approach to prepare "glassy buckypaper" and the solid state reaction for the synthesis of SiC has the advantages of easy operation, scalability, and potentially low-cost production. Moreover, it prevents the waste of Si precursors because the sodium silicate solution used in each synthesis can be recycled and reused.

2. EXPERIMENTAL SECTION

Materials. Pristine single-walled carbon nanotubes (SWNTs, P2) were obtained from Carbon Solutions, Inc. Multiwalled carbon nanotubes (MWNTs) were obtained from Bayer MaterialScience, Inc. Sodium metasilicate, *n*-hydrate ($Na_2SiO_3 \cdot 9H_2O$) was purchased from J T Baker, Inc. All organic solvents were purchased from Sigma Aldrich and used as received. High purity argon and hydrogen gas cylinders (Grade 5.0) were purchased from Valley National Gas, Inc.

Preparation of "Buckypaper" and "Glassy Buckypaper". Single-walled carbon nanotubes (SWNTs, 10.0 mg) were suspended in ethanol (10.0 mL) by 15 min of sonication (Branson 5510 bath sonicator). The suspension was filtered (with PTFE filter, 2 μm) and then washed with DI water (5 mL × 3) and then ethanol (5 mL × 3). A continuous and rigid SWNT network thin film (known as "buckypaper") was formed on top of the filter membrane after this process. While still on the filter, the "buckypaper" of SWNTs was subsequently washed with 0.1 M Na_2SiO_3 aqueous solutions (2 mL × 5). The as-prepared SWNT−silicate composite maintained a film structure and was then collected and dried in an oven at 120 °C overnight. A digital photograph image of the resulting composite film, designated as "glassy buckypaper", is demonstrated in Scheme 1.

Synthesis of SiC Nanorods. The "glassy buckypaper" was placed in the middle of an alumina tube inside a tube furnace (CM Furnaces, Inc.). A gas mixture (800 sccm of Ar flow mixed with 50 sccm of H_2 flow) was introduced into the alumina tube to create the reaction environment. The temperature of the furnace was increased to 1300 °C and was kept for different time periods from 1 to 10 h. After 10 h of reaction at 1300 °C, the product was then burned in air at 700 °C for 3 h to remove all the unreacted carbon to afford SiC nanorods. Alternative synthesis conditions of 1500 °C for 1 h resulted in a similar SiC nanorod product. SiC product synthesized under these conditions required no further thermal treatment. Scheme 1 illustrates the detailed processes of this synthetic approach.

Synthesis of SiC Nanowires. The "glassy buckypaper" was placed in the middle of an alumina tube inside a tube furnace. A gas mixture (800 sccm of Ar flow mixed with 50 sccm of H_2 flow) was introduced into the alumina tube to create the reaction environment. The furnace was heated to 1400 °C, and the heating was quickly stopped once the temperature reached the desired value (a so-called "fast reaction"). A small amount of SiC nanowires with impurities were produced by this procedure. The product was then burned in air at 700 °C for 3 h to remove all the unreacted carbon species to yield SiC nanowires.

Characterizations. Transmission electron microscopy (TEM) of all the synthesized samples was performed on an FEI Morgagni microscope, operating at an acceleration voltage of 80 keV. High-resolution TEM (HRTEM) images were obtained on a JEOL 2010F high-resolution transmission electron microscope equipped with an energy-dispersive X-ray spectroscopy (EDX) accessory, operating at an accelerating voltage of 200 keV. Scanning electron microscopy (SEM) was performed with a Phillips XL30 FEG microscope equipped with an EDX accessory. X-ray Diffraction (XRD) was performed at a Philips X'pert diffractometer for powder and thin film diffraction.

Electrical Measurements of SiC Nanorods. An aqueous suspension of SiC nanorods (0.01 mg/mL) was drop-cast (10 μL × 10) onto a ceramic chip (dense aluminum oxide) with interdigitated platinum electrodes (4 mil spacing, from Electronics Design Center, Case Western Reserve University). Two high-temperature wires with Nextel fiber insulation (maximum working temperature 980 °C, from Omega Engineering, Inc.) were employed as the conducting wires and were connected to a Keithley SourceMeter 2400. The connection between the chip and high-temperature wires was established by wrapping a thin platinum wire around the end of the high-temperature wire; the other end of the thin wire was kept in touch with electrodes on the chip and fixed with platinum−silver paint (maximum working temperature around 600 °C, ESL ElectroScience). The maximum working temperature of such a device was up to 600 °C and could reach up to 1000 °C with a proper platinum paint. Utilizing this system, we managed to measure the *I*−*V* characteristics of the SiC nanorod devices from room temperature to 600 °C in 100 degree intervals in the Ar environment (bias voltage from −20 to 20 V); each temperature was maintained for half an hour before each electrical test. Field-effect transistors (FETs) were also fabricated from the SiC nanorods. Specifically, a small amount of SiC nanorods (0.5 μL of 0.01 mg/mL aqueous suspension) were deposited on top of a Si chip with an oxide layer (300 nm) and interdigitated gold electrodes (from MEMS and Nanotechnology Exchange). The back gate of the chip was attached to a conducting alumina tape through silver paint, and the whole device was taped on top of a glass slide. The FET characteristics of the SiC nanorod device were measured with a Probe Station Micromanipulator that was connected to Keithley SourceMeter 2400,

dx.doi.org/10.1021/am3031008 | ACS Appl. Mater. Interfaces 2013, 5, 1928−1936

and the temperature of the device was controlled by a hot plate, from room temperature to 400 °C in air.

3. RESULTS AND DISCUSSIONS

Figure 1a shows a typical SEM image of the as-prepared SWNT−silicate composite film ("glassy buckypaper"). At relatively low temperatures (1000−1200 °C), no reaction between SWNTs and silicate took place, and no SiC was produced. However, an aggregation of silicate on the side walls of SWNTs was observed, and nanoparticles composed of Si and O were formed (Figure 1b and c). When the calcination temperature was raised to 1300 °C, SWNTs started to react with silicate, and the phase of SiC could be gradually observed, as indicated by the XRD and EDX results (Figure 2a and b).

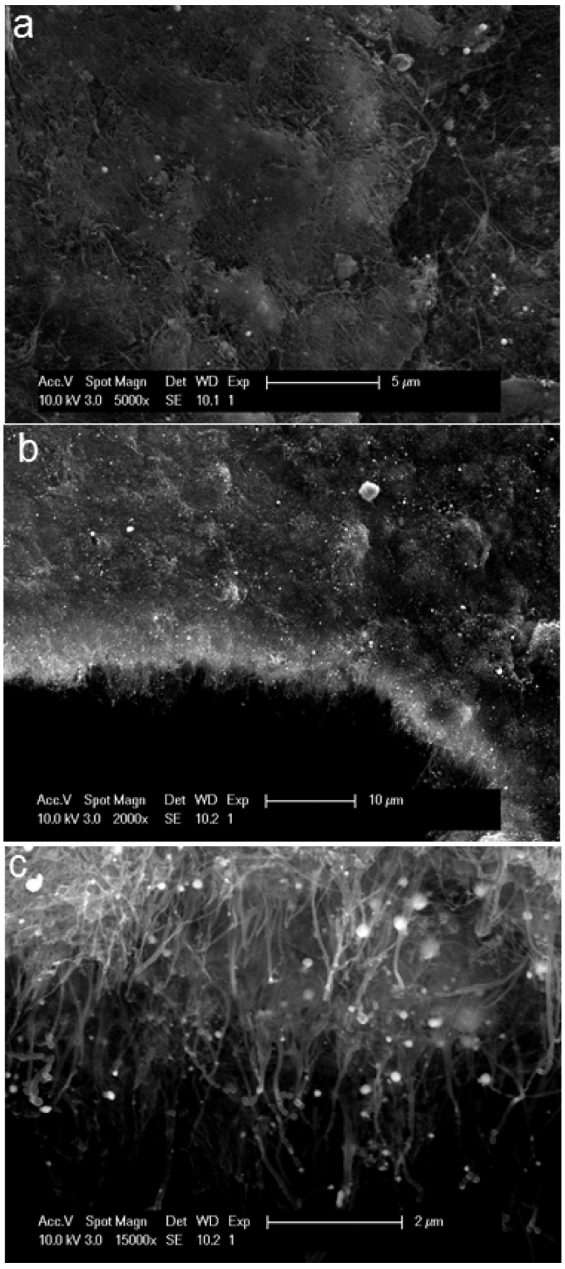

Figure 1. (a) Scanning electron microscopy (SEM) image of a SWNT−silicate film ("glassy buckypaper"). (b,c) SEM images after low-temperature calcination (1200 °C) of "glassy buckypaper".

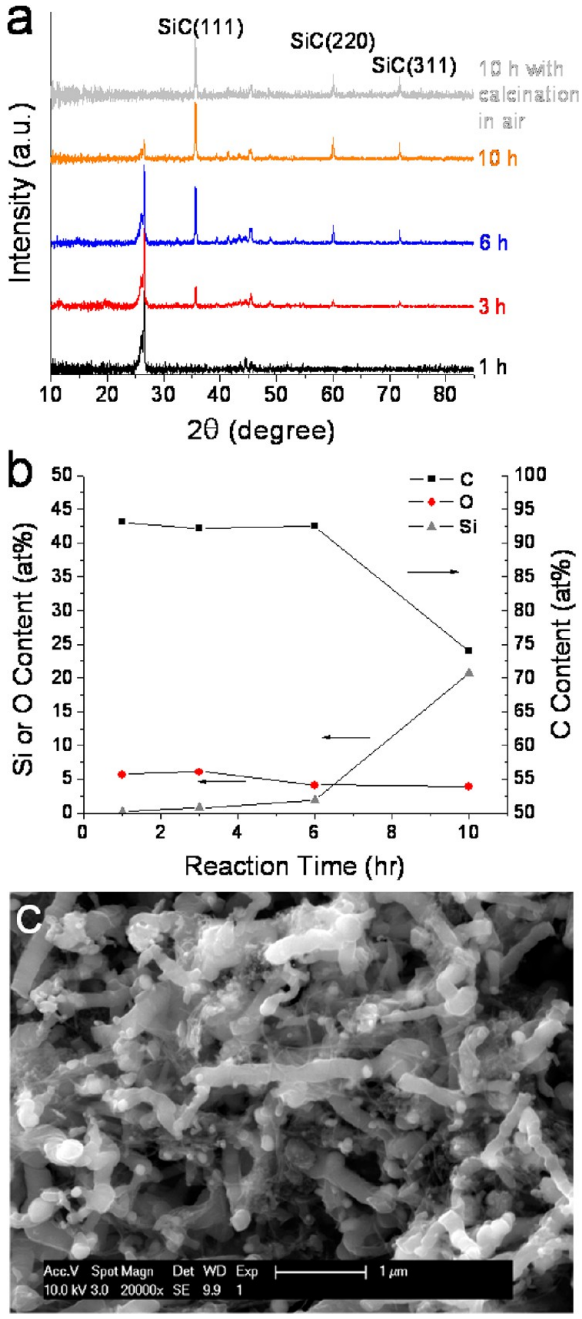

Figure 2. (a) X-ray diffraction (XRD) patterns of the SiC products after different times of calcination at 1300 °C and after calcination at 700 °C in air. The intensity of graphitic peaks (around 27°) gradually decreased with the increasing reaction time, while intensities of the SiC peaks (corresponding to 111, 220, and 311 surfaces of 3C−SiC) increased. After calcination in air, the C residues could be completely removed, resulting in pure SiC product. (b) Energy-dispersive X-ray spectroscopy (EDX) analysis of the SiC products after different times of calcination at 1300 °C. (c) Scanning electron microscopy (SEM) image of the SiC nanorods.

After 10 h of calcination, the reaction was close to completion, and the residue carbon could be removed by an additional calcination in air which was confirmed by XRD (Figure 2a). As also revealed by the XRD spectra, the resulting SiC samples had a well-developed cubic (3C-SiC) crystal structure (also known as β-SiC). Multiple orientations were indicated by the XRD peaks, where the [111] orientation appeared to be predom-

dx.doi.org/10.1021/am3031008 | ACS Appl. Mater. Interfaces 2013, 5, 1928−1936

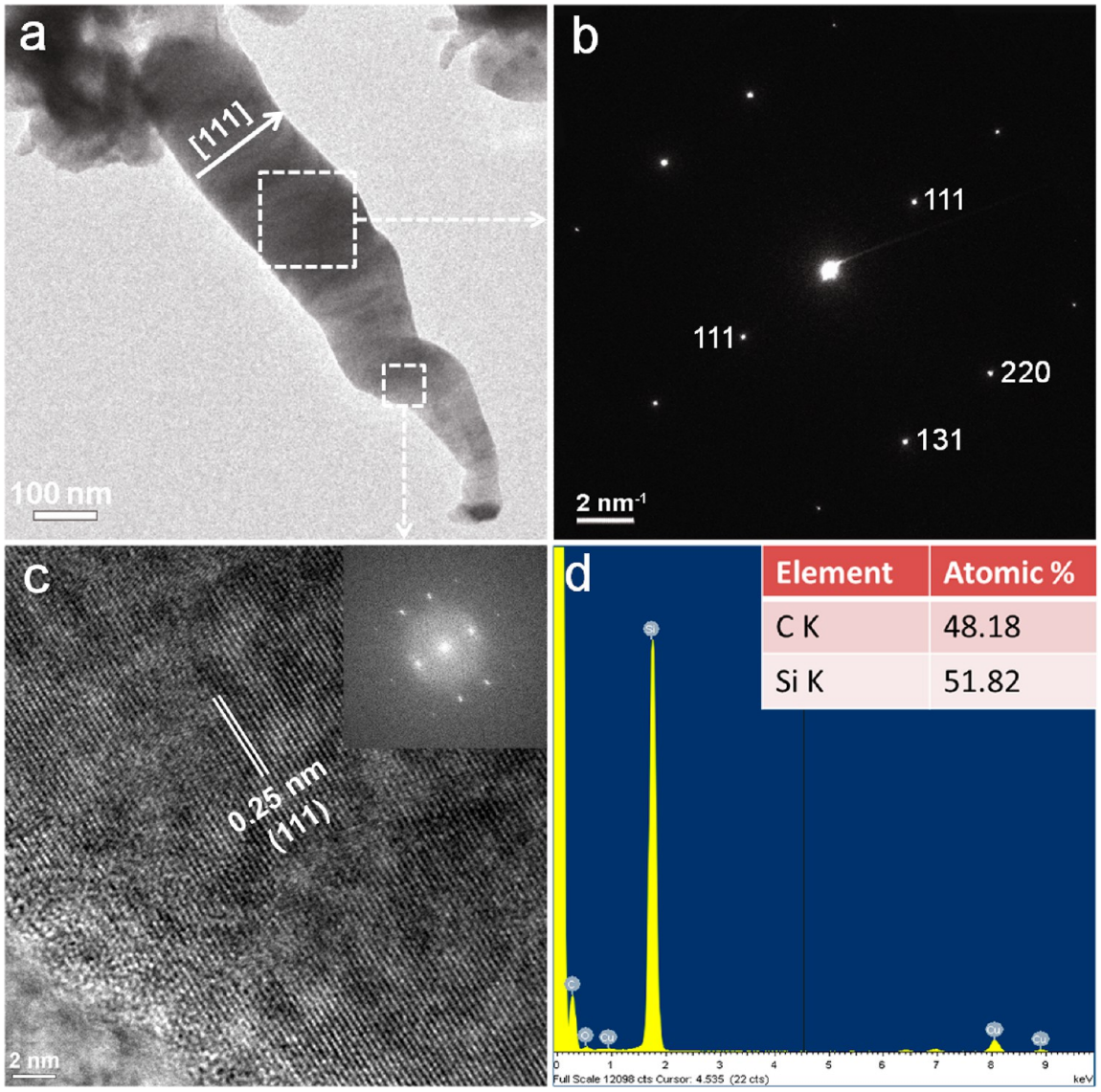

Figure 3. (a) Transmission electron microscopy (TEM) image of a typical SiC nanorod. (b) Selected area electron diffraction (SAED) patterns corresponding to the dashed area in (a), showing a single crystalline structure the same as β-SiC. (c) High-resolution TEM (HR-TEM) image of the selected (dashed) area of the SiC nanorod in (a). The lattice spacing is 0.25 nm, in accordance with the (111) surface lattice of β-SiC. Inset depicts the fast fourier transform (FFT) diffraction patterns of the image. (d) Energy dispersive X-ray spectra (EDX) of the SiC nanorod. Inset depicts the C and Si atomic ratio within the nanorod.

inant. The reaction rate could be further increased by employing a higher calcination temperature. For example, the complete reaction between SWNTs and silicate could be accomplished within 1 h at 1500 °C. However, at this temperature, a lower yield of SiC materials (15 wt % vs 20 wt % for 10 h at 1300 °C) was observed. This was probably due to the volatilization and decomposition of SiC at such high temperatures in a reducing environment.[31] Figure 2c depicts a typical SEM image of the products after calcination of the "glassy buckypaper" at 1300 °C for 10 h. The resulting SiC products were in the form of nanorods with approximately 100 nm in diameter and 1 μm in length, which is also shown in the TEM images (Figure 3a and Figure 4a and e). These characterization results provide evidence that a solid state reaction was enabled to form 1-D SiC nanomaterials through the employment of "glassy buckypaper" with SWNTs as the C source and silicate as the nontoxic Si source. This reaction is different from the generally reported vapor−liquid−solid (VLS) or vapor−solid (VS) mechanism. As a result of the solid-state reaction, the material processing was simplified during the synthesis. Therefore, this "glassy buckypaper" approach may lend itself well to large-scale production.

As a control experiment, multiwalled carbon nanotubes (MWNTs) were also used to form a MWNT−silicate composite to obtain the SiC products. Although MWNTs have elemental composition similar to SWNTs and possess 1-D morphology, SiC nanorods were not formed (see Supporting Information Figure S1). The specific requirement of SWNTs in this synthetic approach was probably due to two reasons. First, SWNTs could easily form a rigid solid film containing the adsorbed silicate (i.e., the "glassy buckypaper"). This could be a key factor to maintain the structural integrity of the nanotubes during the high-temperature solid state reaction to produce SiC. As for MWNTs, large particles were formed instead of a continuous film after they were washed with silicate solutions under the same conditions. Second, as the Si source in this

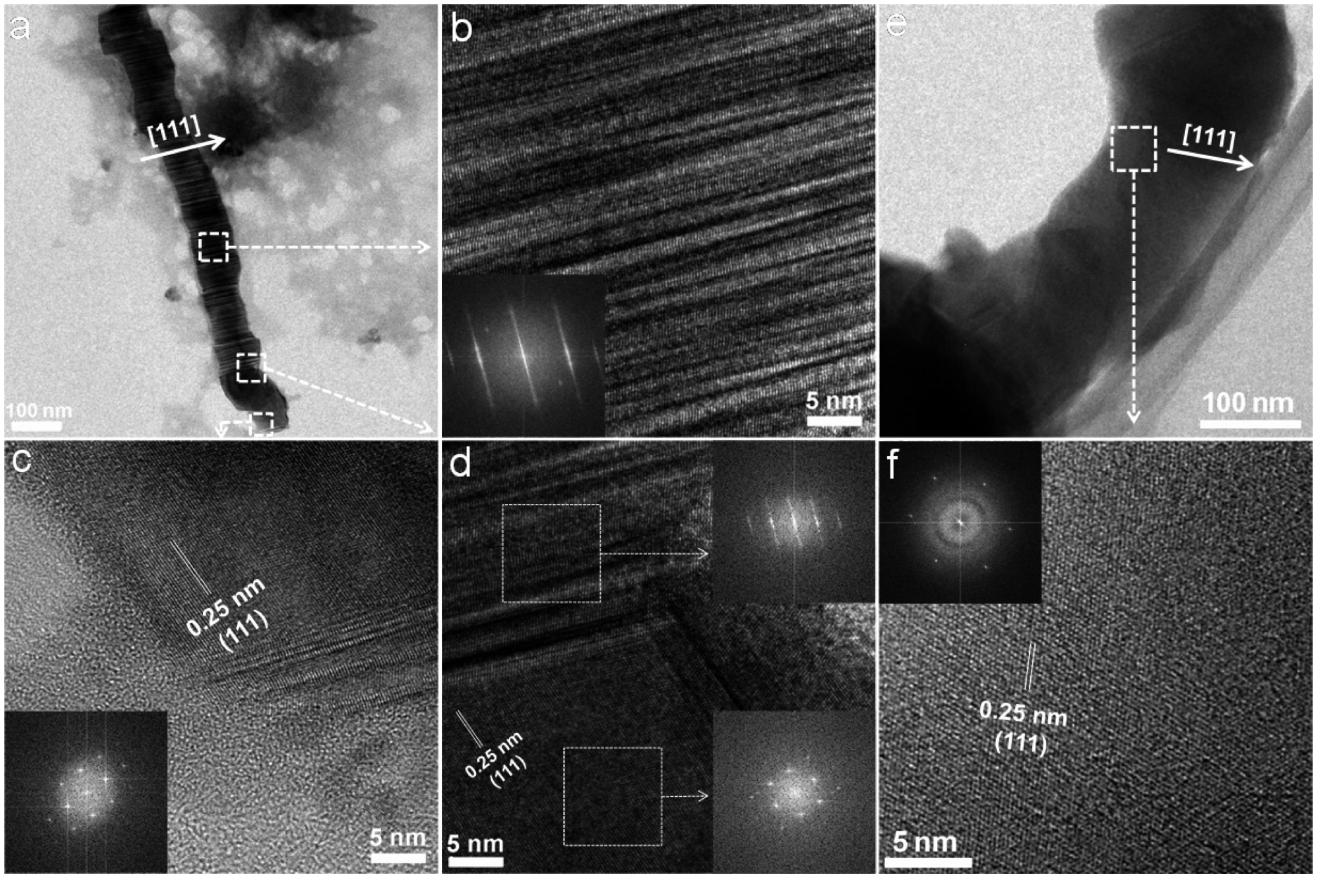

Figure 4. Structural analysis of different SiC nanorods. (a) TEM image of a long SiC nanorod with mostly stacking faults structure. (b, c, d) Corresponding HR-TEM images of the selected area of the nanorod in (a). Insets depict the respective FFT diffraction patterns of each area. (e) TEM image of a short SiC nanorod with 3C−SiC structure. (f) HR-TEM image of the selected area in (e); inset depicts the FFT diffraction pattern of the image.

approach was from the silicate adsorbed on the surface of carbon nanotubes, the corresponding C source was only necessary from the surface C atoms. While SWNTs were entirely composed of surface atoms, inner tubes of MWNTs provided an excess of C during the reaction. The extra C could undergo a variety of possible reactions, and these subsequent reactions were overall not beneficial for maintaining the existing 1-D morphology.

The morphology and crystal structure of SiC nanorods synthesized from the "glassy buckypaper" were further studied in detail. Figure 3a shows a TEM image of a typical SiC nanorod, and electron diffraction patterns of the selected area of this nanorod (top dashed rectangular part in Figure 3a) are demonstrated in Figure 3b. The selected area electron diffraction (SAED) patterns indicated that the SiC nanorod was single crystalline, with a well-developed 3C−SiC crystal structure.[32] This was further confirmed by the high-resolution TEM (HR-TEM) imaging of the same nanorod (Figure 3c), where the interfringe distance of the lattice was determined to be 0.25 nm, in agreement with (111) lattice spacing of the 3C−SiC. The corresponding fast Fourier transformed (FFT) diffraction patterns are also demonstrated as the inset of Figure 3c. It could be noticed that the FFT patterns revealed the same structural information as the SAED patterns, and they were thus employed in the following structural analysis (such as in Figure 4). The detailed crystal structures of the SiC nanorod were consistent with the conclusion obtained from the bulk XRD results (Figure 2a). Furthermore, EDX analysis of the single SiC nanorod indicated that it contained C and Si elements with an atomic ratio that was close to 1:1, as shown in Figure 3d.

While most SiC nanorods synthesized from "glassy buckypaper" exhibited crystal structures similar to that in Figure 3a, other morphology was present. Figure 4a demonstrates a relatively long nanorod with disordered or defective structure that could be attributed to the stacking faults (SFs), as shown in Figure 4b.[33,34] Long streaks resulting from the stacking faults[33] were further observed in the FFT diffraction patterns (Figure 4b inset). The end point of the nanorod appeared to be single crystalline, as shown in Figure 4c and d, which could probably serve as the starting point for the growth of the SF regions. The interface between two different regions is demonstrated in Figure 4d, where the transition from single crystalline to the highly disordered SF area occurred at a bend in the nanorod. It should be mentioned that such nanorods with high SF ratios were not commonly observed in the bulk nanorod sample, as also indicated by the lack of a SF diffraction peak[8,33] in the bulk XRD result (Figure 2a). Another typical single crystalline 3C−SiC nanorod that was representative to the sample is demonstrated in Figure 4e and 4f.

The cubic (3C) crystal structure of SiC nanorods was similar to a variety of previously reported SiC nanowires.[8,22,23] However, a [111] lattice orientation that was perpendicular to the longitudinal axes of the nanorods was observed in our sample, as illustrated in Figures 3a, 4a, and 4e, and was further confirmed by the lattice lines observed in the HR-TEM image

and corresponding SAED/FFT patterns. This orientation was different from the most reported structures of SiC nanowires, where the [111] direction was usually along the growth direction of the nanowires.[8,22,23,32−35] This unusual orientation has probably resulted from our unique synthetic approach from "glassy buckypaper", where formation and growth of SiC nanorods originated from pure solid state reactions.

Although the resulting SiC nanorods maintained the one-dimensional structure of SWNTs, the nanorods were shorter in length and larger in diameter, compared with the starting nanotube templates. Two possible reasons are proposed here to explain such a difference in the morphology. First, the SWNT template existed as bundles in the network, with a diameter larger than the individual nanotube. Second, the aggregation of silicate precursors on the carbon nanotube started from a temperature (1200 °C, Figure 1c) lower than the reaction temperature (1300 °C) and could last during the long time of reaction (10 h). It should also be noted that it took approximately 30 min for the furnace to heat to a temperature of 1200 °C or higher. Therefore, adsorbed silicate aggregated to form bigger particles along SWNTs before temperature became high enough for the formation of SiC. After the nanoparticles were formed and temperature reached 1300 °C, the reaction started from the interface between carbon nanotube bundles and silicate particles, with further material migration before the complete formation of SiC. As a result, shorter SiC nanorods with larger diameters were formed. To minimize silicate aggregation and obtain one-dimensional SiC nanostructures with higher length to diameter ratio (ideally to be similar to the starting carbon nanotubes), another fast calcination strategy was employed. In this alternative method, the furnace containing the SWNT−silicate composite film was heated to a temperature higher than 1300 °C (typically 1400 °C), and the heating was stopped immediately after the furnace reached the desired temperature. As shown in Figure 5 (method 2), the furnace temperature reached a peak value and then started to drop instantly. With this specific heating strategy, the "glassy buckypaper" experienced a much shorter period of heating, and the aggregation of the silicate was minimized. On the other hand, the high-temperature region that might cause the volatilization and decomposition of SiC products was also limited. The comparison of detailed temperature profiles between these two methods is demonstrated in Figure 5. Overall, compared with the former increasing and constant "step-shaped" heating, this alternative "peak-shaped" heating method was expected to give a better length to diameter ratio of the final SiC nanostructures.

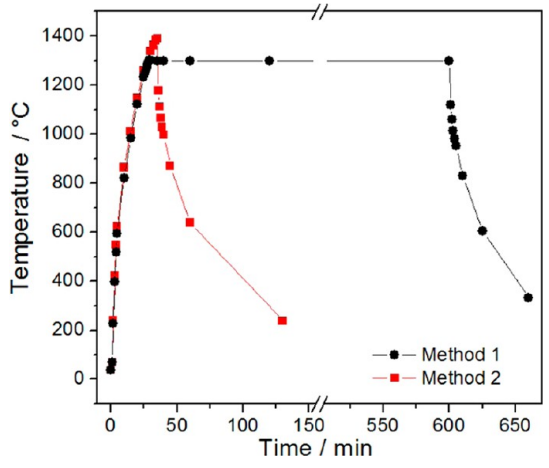

Figure 5. Temperature profiles of two different calcination approaches for the production of SiC nanostructures. Method 1 led to the formation of SiC nanorods, whereas method 2 led to the formation of SiC nanowires.

As shown in Figure 6a, this fast heating approach indeed generated a SiC nanowire product with longer length (several micrometers) and smaller diameters (10−50 nm). Due to the shorter reaction times, these as-prepared SiC nanowires appeared to be amorphous in crystallinity (Figure 6b). We further noticed that due to the short period of calcination there is an aggregation of metal species in the material network, which resulted in some metal nanoparticle impurities in the final products (Figure S2, Supporting Information). These metal residues probably originated from the catalysts that were used to produce SWNTs, as different metal nanoparticles were generated from different carbon nanotube sources (Ni nanoparticles from arc discharge, Carbon Solutions, Inc., and Fe nanoparticles from HiPCO, Carbon Nanotechnologies Inc., Figure S2, Supporting Information). These nanoparticles were not observed in the SiC nanorod samples, probably due to the long calcination time in the hydrogen gas environment. Therefore, further calcination and chemical treatments were required to produce highly crystalline and pure SiC nanowires.

On the basis of the aforementioned material characterization results, we can propose a two-step mechanism for the formation of 1-D SiC nanostructures from "glassy buckypaper" as summarized in Figure 7. This silicate-coated SWNT architecture, formed during the silicate washing of the SWNT network, has an ideal structure that utilizes the morphology of SWNTs as templates with a large reaction interface for the formation of SiC of commensurate dimensions. However, two competing processes can occur during the calcination of this "glassy buckypaper" network: At the low-temperature region (below 1200 °C), silicate coatings start to aggregate, while no reaction with SWNTs takes place. When the temperature reaches a relatively high value (above 1300 °C), SiC is gradually produced from the reaction between C and the Si source. Since the reaction could only occur at the SWNT−silicate interface, the final morphology of the SiC product is therefore determined by the size of the aggregated Si-containing particles. As a result of the competition between the silicate aggregation and C−Si reaction, control of the temperature profiles (most importantly, the rate of heating) could effectively alter the morphology of SiC nanostructures in this synthetic approach. This mechanism can explain our observation of the formation of SiC nanorods and nanowires from the same starting material under different temperature profiles.

SiC-based materials are particularly promising for applications in electrical devices that have to be operated in harsh conditions, such as high temperature, high pressure, and oxidizing environment. The one-dimensional morphology of SiC nanorods or nanowires also made them an ideal candidate for chemical sensing in extreme situations where carbon nanotubes or Si nanowires cannot be employed. Here we fabricated chemiresistive devices based on the one-dimensional SiC nanorods and tested their electrical properties at elevated temperatures. The device schematic is illustrated in Figure 8a. Such electrical devices could be potentially used for gas detection at high temperatures. As shown in Figure 8b and c, the conductivities of the SiC nanorod devices increased with the rising temperatures; however, the relationship between the

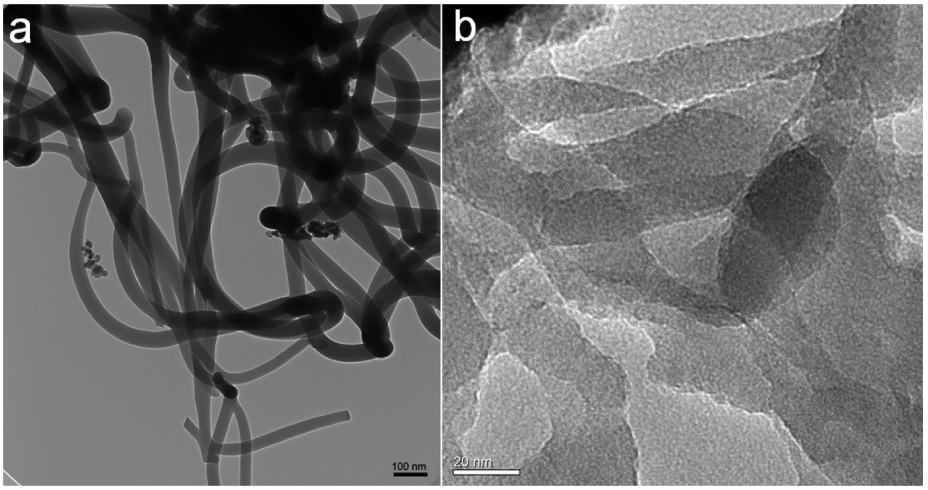

Figure 6. (a) TEM and (b) HR-TEM images of SiC nanowires.

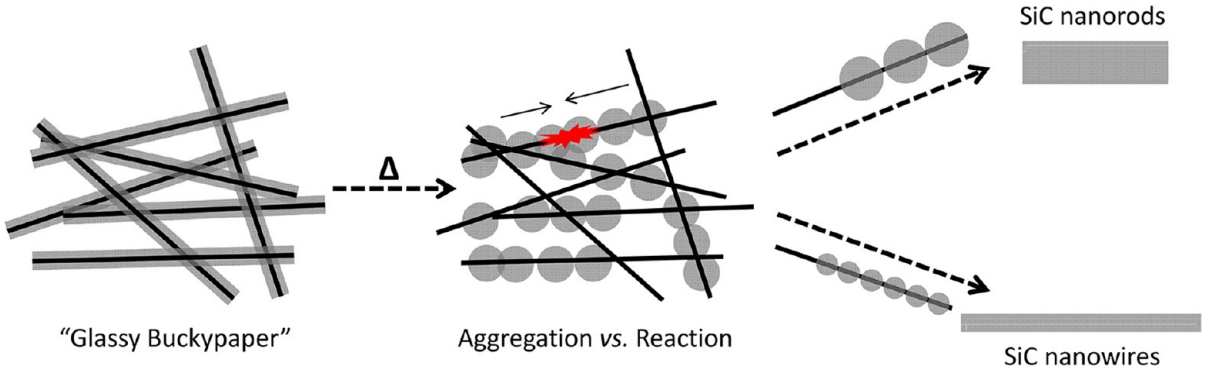

Figure 7. Proposed mechanism for the formation of one-dimensional (1-D) SiC nanostructures from "glassy buckypaper". During the high-temperature calcination, the competition between silicate aggregation and C−Si reaction determines the final morphology of SiC nanostructures. Residual carbon is removed during the subsequent calcination in air.

device resistance and the temperature observed in this work differs from those reported for bulk SiC or SiC nanowires.[6,7] This result indicated that both charge carrier mobility and contact barriers play a role in the change of device performance with varying temperatures. It should also be noted that the average conductance of our SiC nanorod devices was 5 orders of magnitude lower than the reported conductance of single β-SiC nanowire devices.[6,36] This could be rationalized by two possible reasons: (i) the SiC nanorods prepared in this work were undoped and (ii) the devices were fabricated based on a film of numerous SiC nanorods. Compared with single SiC nanowire devices, a much longer charge carrier pathway and significant amount of nanorod−nanorod interconnections could both contribute to the much higher resistivity. The increased resistance was not a critical problem for the use of SiC nanorods in a chemiresistor that has less strict requirements on device conductance; on the other hand, the abundance of rod to rod interconnections in the device could actually be beneficial for the potential sensor applications, as it has been reported that resistance determined by interface between 1-D nanostructures could provide additional chemical sensitivity.[37] Moreover, a field-effect transistor was fabricated from SiC nanorods, where the back gate of the device was attached through silver paint to a conducting alumina tape, and all the electrodes (source, drain, and gate) were connected to a probe station micromanipulator. The $I-V_g$ curves of a SiC nanorod device are shown in Figure S4 (Supporting Information). Due to the low density of nanorods in the device, low source−drain current was observed during the scanning of gate voltage at room temperature. At elevated temperatures, p-type semiconductor characteristics were observed. This result was unexpected since no dopant was intentionally added during the synthetic process; moreover, unintentional doping usually resulted in n-type SiC nanostructures.[38,39] The possible source of p-type unintentional doping could be either Al[40] from the alumina container or other metal residues left from SWNTs, and further investigation will be required for clarification. Overall, the electrical measurements of SiC nanorods demonstrated their potential to be incorporated into electrical devices with promising future applications in the high-temperature chemiresistor for chemical sensing in the specific environment.

4. CONCLUSIONS

In summary, we have developed a simple, scalable, and low-cost approach for the synthesis of one-dimensional SiC nanostructures using carbon nanotubes as templates. Compared with generally used vapor−liquid−solid (VLS) and vapor−solid (VS) reactions based on Si containing vapors, the employment of "glassy buckypaper" and the following solid state reaction will significantly simplify the material processing and reduce the production cost. EDX and XRD characterizations confirmed the successful synthesis of SiC material using this approach. SEM and TEM characterizations demonstrated their one-

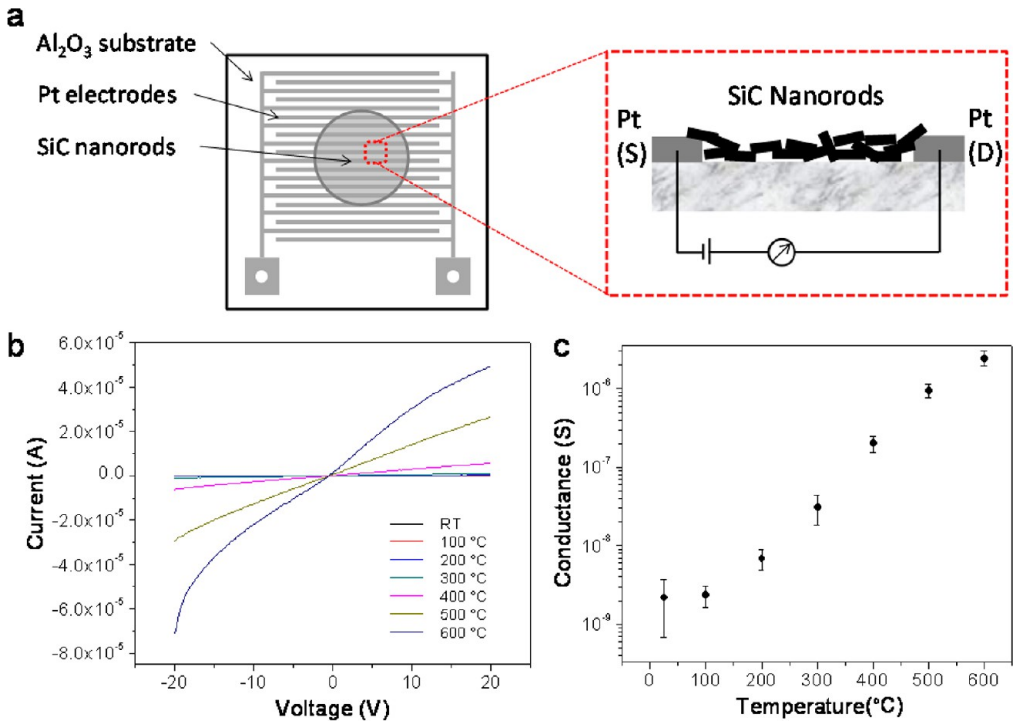

Figure 8. Electrical characterization of the SiC nanorod devices. (a) Schematic representation of the electrical device fabricated from SiC nanorods. (b) *I*–*V* characteristics of the SiC nanorod devices at different temperatures from room temperature to 600 °C. (c) Conductance of the SiC nanorods at different temperatures.

dimensional morphology and detailed crystal structure and orientation. The final morphology of SiC nanomaterials was determined by programming of the heating procedure, and two 1-D nanostructures, SiC nanorods, and SiC nanowires were obtained from two different heating profiles. Such correlation inspired a future direction where extreme heating profiles (such as fast laser heating) could be utilized for the fabrication of 1-D SiC nanomaterials from the "glassy buckypaper" with better controlled morphology. Although the quality of SiC nanowires was limited due to the catalyst residues in the commercial SWNT samples, it could be expected that this approach will provide an innovative and practical way of producing SiC nanowires with similar quality to previously developed methods, once industrial production of SWNTs or "buckypaper" achieved better quality and purity. In addition, electrical devices that could operate at elevated temperatures were successfully fabricated from SiC nanorods, with future applications in chemical sensing at harsh conditions.

■ ASSOCIATED CONTENT

Ⓢ Supporting Information

TEM images of SiC nanostructures produced from MWNTs, TEM images and EDX characterization of SiC nanowires, UV–vis absorption spectra, and photoluminescence emission spectra of SiC nanorods. This material is available free of charge via the Internet at http://pubs.acs.org.

■ AUTHOR INFORMATION

Corresponding Author

*E-mail address: astar@pitt.edu.

Notes

The authors declare no competing financial interest.

■ ACKNOWLEDGMENTS

This work was performed in support of ongoing research in sensor systems and diagnostics at the National Energy Technology Laboratory (NETL) under URS contract DE-FE0004000. We thank the Nanoscale Fabrication & Characterization Facility (NFCF) for the access to the XRD and electron microscopy instrumentations and Dr. Susheng Tan for the assistance with HR-TEM and SAED.

■ REFERENCES

(1) Wright, N. G.; Horsfall, A. B.; Vassilevski, K. *Mater. Today* **2008**, *11*, 16.
(2) *Gmelin Handbook of Inorganic Chemistry: Si*; Springer: Berlin, 1984; Supplement Vol. *B2*, Silicon Carbide, part 1.
(3) *Gmelin Handbook of Inorganic Chemistry: Si*; Springer: Berlin, 1986; Supplement Vol. *B3*, Silicon Carbide, part 2.
(4) Avouris, P. *Acc. Chem. Res.* **2002**, *35*, 1026.
(5) Lu, W.; Lieber, C. M. *J. Phys. D: Appl. Phys.* **2006**, *39*, R387.
(6) Zekentes, K.; Rogdakis, K. *J. Phys. D: Appl. Phys.* **2011**, *44*, 133001.
(7) Zhou, W. M.; Fang, F.; Hou, Z. Y.; Yan, L. J.; Zhang, Y. F. *IEEE Electron. Device Lett.* **2006**, *27*, 463.
(8) Li, Z.; Zhang, J.; Meng, A.; Guo, J. *J. Phys. Chem. B* **2006**, *110*, 22382.
(9) Xie, Z.; Tao, D.; Wang, J. *J. Nanosci. Nanotechnol.* **2007**, *7*, 647.
(10) Li, G.; Li, X.; Wang, H.; Liu, L. *Appl. Phys. A: Mater. Sci. Process.* **2010**, *98*, 293.
(11) Niu, J. J.; Wang, J. N.; Xu, Q. F. *Langmuir* **2008**, *24*, 6918.
(12) Kim, H. Y.; Park, J.; Yang, H. *Chem. Commum.* **2003**, *2*, 256.
(13) Seeger, T.; Kohler-Redlich, P.; Ruhle, M. *Adv. Mater.* **2000**, *12*, 279.
(14) Li, Y. B.; Xie, S. S.; Zou, X. P.; Tang, D. S.; Liu, Z. Q.; Zhou, W. Y.; Wang, G. *J. Cryst. Growth* **2001**, *223*, 125.
(15) Zhang, X.; Chen, Y.; Xie, Z.; Yang, W. *J. Phys. Chem. C* **2010**, *114*, 8251.

(16) Wu, R.; Yang, G.; Gao, M.; Li, B.; Chen, J.; Zhai, R.; Pan, Y. *Cryst. Growth Des.* **2009**, *9*, 100.
(17) Wang, H.; Lin, L.; Yang, W.; Xie, Z.; An, L. *J. Phys. Chem. C* **2010**, *114*, 2591.
(18) Gundiah, G.; Madhav, G. V.; Govindaraj, A.; Seikh, M. M.; Rao, C. N. R. *J. Mater. Chem.* **2002**, *12*, 1606.
(19) Yang, Z.; Xia, Y.; Mokaya, R. *Chem. Mater.* **2004**, *16*, 3877.
(20) Niu, J. J.; Wang, J. N.; Xu, Q. F. *Langmuir* **2008**, *24*, 6918.
(21) Yang, Y.; Meng, G.; Liu, X.; Zhang, L.; Hu, Z.; He, C.; Hu, Y. *J. Phys. Chem. C* **2008**, *112*, 20126.
(22) Ye, H.; Titchenal, N.; Gogotsi, Y.; Ko, F. *Adv. Mater.* **2005**, *17*, 1531.
(23) Zhou, W. M.; Liu, X.; Zhang, Y. F. *Appl. Phys. Lett.* **2006**, *89*, 223124.
(24) Zhou, W. M.; Yan, L. J.; Wang, Y.; Zhang, Y. F. *Appl. Phys. Lett.* **2006**, *89*, 013015.
(25) Dai, H.; Wong, E. W.; Lu, Y. Z.; Fan, S.; Lieber, C. M. *Nature* **1995**, *375*, 769.
(26) Liu, J. W.; Zhong, D. Y.; Xie, F. Q.; Sun, M.; Wang, E. G.; Liu, W. X. *Chem. Phys. Lett.* **2001**, *348*, 357.
(27) Pan, Z.; Lai, H. L.; Au, F. C. K.; Duan, X.; Zhou, W.; Shi, W.; Wang, N.; Lee, C. S.; Wong, N. B.; Lee, S. T.; Xie, S. *Adv. Mater.* **2000**, *12*, 1186.
(28) Sun, X. H.; Li, C. P.; Wong, W. K.; Wong, N. B.; Lee, C. S.; Lee, S. T.; Teo, B. K. *J. Am. Chem. Soc.* **2002**, *124*, 14464.
(29) Pham-Huu, C.; Keller, N.; Ehret, G.; Ledoux, M. J. *J. Catal.* **2001**, *200*, 400.
(30) Taguchi, T.; Igawa, N.; Yamamoto, H.; Jitsukawa, S. *J. Am. Ceram. Soc.* **2005**, *88*, 459.
(31) Mendybaev, R. A.; Beckett, J. R.; Grossman, L.; Stolper, E.; Cooper, R. F.; Bradley, J. P. *Geochim. Cosmochim. Acta* **2002**, *66*, 661.
(32) Chen, J.; Tang, W.; Xin, L.; Shi, Q. *Appl. Phys. A: Mater. Sci. Process.* **2011**, *102*, 213.
(33) Zhang, Y.; Han, X.; Zheng, K.; Zhang, Z.; Zhang, X.; Fu, J.; Ji, Y.; Hao, Y.; Guo, X.; Wang, Z. *Adv. Funct. Mater.* **2007**, *17*, 3435.
(34) Bechelany, M.; Brioude, A.; Cornu, D.; Ferro, G.; Miele, P. *Adv. Funct. Mater.* **2007**, *17*, 939.
(35) Li, G.; Li, X.; Chen, Z.; Wang, J.; Wang, H.; Che, R. *J. Phys. Chem. C* **2009**, *113*, 17655.
(36) Lee, K. M.; Choi, T. Y.; Lee, S. K.; Poulikakos, D. *Nanotechnology* **2006**, *21*, 125301.
(37) Ding, M.; Sorescu, D. C.; Kotchey, G. P.; Star, A. *J. Am. Chem. Soc.* **2012**, *134*, 3472.
(38) Seong, H.; Choi, H.; Lee, S.; Lee, J.; Choi, D. *Appl. Phys. Lett.* **2004**, *85*, 1256.
(39) Zhou, W.; Liu, X.; Zhang, Y. *Appl. Phys. Lett.* **2006**, *89*, 223124.
(40) Chen, Y.; Zhang, X.; Zhao, Q.; He, L.; Huang, C.; Xie, Z. *Chem. Commun.* **2011**, *47*, 6398.